

# Impact of Reputation in Multi-Agent Systems Using Master/Slave Methodology

Diogo A. Rosário<sup>1</sup>, João E.M. Raposo<sup>2</sup>, Ketevan<sup>3</sup> Luís Macedo<sup>4</sup>,

<sup>1</sup>University of Coimbra, CISUC - Centre for Informatics and Systems of the University of Coimbra,  
Department of Informatics Engineering, Coimbra, Portugal

{uc2023185395@student.uc.pt, uc2023147060@student.uc.pt, xkark027@studenti.czuz.cz}

## Abstract

The integration of agents into the realm of object identification [11] and specialization stands as a captivating avenue of exploration with vast practical implications. Our paramount objective in this study is twofold: to scrutinize the specialization of drones and to delve into the crucial role played by the master in governing these aerial agents. Our focus extends beyond the mere specialization of drones; we are keenly interested in comprehending how the concentration of training on specific object categories impacts the drones' proficiency in accurate object identification. Furthermore, our inquiry is directed towards unraveling the master's influence in harnessing confidence metrics to discern the optimal drones for particular identification tasks. The essence of our research lies in grasping the intricate interplay between drone specialization, master control, and the pragmatic application of confidence metrics in real-world scenarios.

41  
42  
43  
44  
45  
46  
collective efficacy of the system. Through meticulous parameter manipulation, we seek to unravel the dynamics and answer critical questions regarding the functional consequences of reputation value manipulations, ultimately shedding light on the intricate interplay between reputation, trust, and the operational dynamics of AI-driven intelligent agents.

## 2 State of the Art

In this section, our objective is to present the state of the art in our work.

50  
51  
52  
53  
54  
55  
56  
57  
58  
59  
60  
61  
Multi-agent systems have consistently been a focal point in the field of artificial intelligence. Our approach began with an extensive review of existing literature on multi-agent systems within the scientific community. Professor Luís Macedo played a pivotal role by recommending relevant works authored by other researchers and entities for our analysis. We initiated our exploration by scrutinizing several of these pre-existing works, with a specific focus on the report titled "Uncertainty and Novelty-based Selective Attention in the Collaborative Exploration of Unknown Environments." This report, authored by Luis Macedo, Miguel Tavares, Pedro Gaspar, and Amilcar Cardoso[13], served as a foundational reference for our research.

62  
63  
64  
65  
66  
67  
68  
69  
70  
The insights gained from our analysis of this report provided inspiration for the conceptualization of the ideas detailed in this document. In addition to reviewing the existing literature, we also investigated the latest advances, technologies, and current methods in the field of multi-agent systems. This exploration allowed us to incorporate contemporary approaches into our research, ensuring that our work is situated at the forefront of current developments.

71  
72  
73  
74  
75  
While recent progress has propelled the field forward, it is crucial to acknowledge the presence of unresolved challenges. The identification of these challenges not only informs the current state of the art but also lays the groundwork for potential avenues of future research.

## 3 Materials

### Overview of Roboflow

77  
78  
79  
80  
81  
Roboflow [19] stands out as a pivotal component in our project, serving as an integral platform for preprocessing and managing datasets to facilitate the training of machine learning models. It is a cloud-based service designed to stream-

1  
2  
3  
4  
5  
6  
7  
8  
9  
10  
11  
12  
13  
14  
15  
16  
17  
18  
19  
20  
21  
22  
23  
24  
25  
26  
27  
28  
29  
30  
31  
32  
33  
34  
35  
36  
37  
38  
39  
40  
41  
42  
43  
44  
45  
46  
47  
48  
49  
50  
51  
52  
53  
54  
55  
56  
57  
58  
59  
60  
61  
62  
63  
64  
65  
66  
67  
68  
69  
70  
71  
72  
73  
74  
75  
76  
77  
78  
79  
80  
81

## 1 Introduction

21 In the realm of artificial intelligence (AI) systems, the measure of trust encapsulated within the concept of reputation holds paramount significance in fostering efficient connections. This project centers around the intricate modification 22 of reputation values assigned to individual drones within a meticulously controlled simulation environment. Serving as 23 intelligent agents with predefined tasks, these drones operate 24 within a reputation-based framework, where the project's core 25 objective is to unravel the consequences ensuing from alterations 26 in their reputation values. In this context, high 27 reputation values render drones more likely to be trusted and chosen 28 for tasks, while lower values may invoke skepticism or avoidance. The project explores the nuanced dynamics of 29 reputation, recognizing its pivotal role in shaping the behavior 30 and interactions of intelligent agents. With a primary focus 31 on testing the master control system's outcomes, we aim 32 to investigate the impact of reputation value alterations on the 33 overall process. By engaging in systematic experiments, our 34 objective is to discern how changes in reputation values influence 35 not only individual drone performance but also the

82	line the end-to-end process of computer vision model development.	136
83		137
84	<b>Utilization and Applications</b>	138
85	The primary usage of Roboflow in our project revolves around data preprocessing, annotation, and the generation of augmented datasets. By employing Roboflow's user-friendly interface, we were able to seamlessly organize and annotate our dataset, ensuring its compatibility with various computer vision models.	139
86		140
87		141
88		142
89		
90		
91	<b>YOLOv8 Architecture</b>	143
92	Roboflow employs the YOLOv8 [10][12] (You Only Look Once, Version 8) architecture as a cornerstone for object detection tasks in model training. YOLOv8 represents an evolution of the YOLO series, incorporating advancements in architecture design for improved accuracy and efficiency. This model is characterized by its ability to process images in real-time while maintaining high detection performance. The figure illustrating architecture of the YOLOv8 model [10] is located in the attached sheets at the end of this report as Figure 4.	144
93		145
94		146
95		147
96		148
97		149
98		150
99		
100		
101		
102	<b>Integration with COCO Dataset</b>	151
103	Integral to the efficacy of YOLOv8 within Roboflow is its training on the COCO (Common Objects in Context) dataset. The COCO dataset [9], renowned for its extensive image collection across 80 object categories, serves as a robust foundation for training YOLOv8 to recognize and localize objects accurately. The seamless integration of COCO within Roboflow enhances the model's capacity for generalization across diverse scenarios.	152
104		153
105		154
106		155
107		156
108		157
109		
110		
111	<b>Data Augmentation Strategies</b>	158
112	Roboflow employs sophisticated data augmentation strategies during the training process, contributing to the versatility and robustness of the YOLOv8 model. Techniques such as rotation, flipping, and adjustments in brightness and contrast are systematically applied to augment the training dataset. This augmentation process enhances the model's ability to handle variations in real-world scenarios effectively.	159
113		160
114		161
115		162
116		163
117		164
118		165
119	<b>Transfer Learning for Model Optimization</b>	166
120	A pivotal aspect of Roboflow's training mechanism is the incorporation of transfer learning. YOLOv8, initially pre-trained on a comprehensive dataset like COCO, undergoes fine-tuning on the specific dataset pertinent to our project. This transfer learning approach allows the model to leverage knowledge gained from a broader dataset and adapt it to the intricacies of the target dataset, ensuring rapid convergence and enhanced performance.	167
121		168
122		169
123		170
124		
125		
126		
127		
128	<b>Hyperparameter Tuning</b>	
129	Roboflow's model training pipeline includes meticulous hyperparameter tuning. Parameters such as learning rates, batch sizes, and optimization algorithms are systematically adjusted to optimize the YOLOv8 model's performance on the specific detection task. This fine-tuning process ensures a balanced trade-off between precision and computational efficiency.	
130		
131		
132		
133		
134		
135		

## 171 4 Datasets

### 172 4.1 Treatment

173 The datasets employed to train each drone consist of a varying  
174 number of distinct images. Emphasis is also given to the  
175 labels presented in each image, with the number of labels differ-  
176 ing for each dataset. The composition of each dataset is as  
177 follows:

#### 178 Drone A

179 Drone A employed 498 images[3] including 298 of cars with  
180 20,389 labels[6], 100 of trees with 3,628 labels[14], and 100  
181 of houses with 850 labels[17]. The total number of labels in  
182 this dataset is 24,867. This drone was trained with this dataset  
183 composition, as the experimental aim was for it to be the most  
184 proficient in identifying cars.

#### 185 Drone B

186 Drone B employed 1,610 images[4], including 200 of cars with  
187 8,876 labels[2], 427 of trees with 24,979 labels[20], and  
188 974 of houses with 2,000 labels[1]. The total number of labels  
189 in this dataset is 34,055. This drone was trained with this  
190 dataset composition, as the experimental aim was for it to be  
191 the most proficient in identifying houses.

#### 192 Drone C

193 Drone C employed 432 images[5], including 50 of cars with  
194 3,085 labels[7], 182 of trees with 15,052 labels[21], and 200  
195 of houses with 906 labels[15]. The total number of labels in  
196 this dataset is 19,043. This drone was trained with this dataset  
197 composition, as the experimental aim was for it to be the most  
198 proficient in identifying trees.

## 199 5 Methods

200 After the image selection process, training for each drone be-  
201 gins by choosing between two training models:

- 202 • Accurate (used in all cases): It is slower to train and infer,  
203 aiming to achieve a more precise drone in identifying  
204 specific objects.
- 205 • Fast: A training model that is quicker to train and infer  
206 than the former but is less accurate.

207 Following this initial choice, the decision is made to use  
208 the YOLOv8 architecture with integration from the COCO  
209 dataset. After this last decision, the dataset division for train-  
210 ing, testing, and validation is presented as follows:

- 211 • For Drone A, 73% of the total images are used for the  
212 training set, 16% for the validation set, and 11% for the  
213 testing set.
- 214 • For Drone B, 71% of the total images are used for the  
215 training set, 14% for the validation set, and 15% for the  
216 testing set.
- 217 • For Drone C, 75% of the total images are used for the  
218 training set, 19% for the validation set, and 6% for the  
219 testing set.

220 These datasets, featuring varying image sizes and different  
221 numbers of images for each set, aimed to isolate the ex-  
222 perience of each drone. Consequently, three drones were ob-  
223 tained, each possessing distinct levels of expertise in object  
224 identification.

225 A pre-processing step is also presented, involving auto-  
226 orientation of images for all drones and the possibility of re-  
227 sizing each image in the datasets. Specific resize dimensions  
228 were applied for each drone:

- 229 • For Drone A, a resize of 500x500 was used.
- 230 • For Drone B, a resize of 640x640 was applied.
- 231 • For Drone C, a resize of 400x400 was implemented.

232 Regarding data augmentation strategies, as mentioned in  
233 Section 2.1 on Roboflow Integration and Model Training,  
234 Roboflow provides various augmentation strategies. For each  
235 of the drones, no augmentation was applied.

236 After training each drone, the following results are pre-  
237 sented concerning mAP(Average Precision Metric), Preci-  
238 sion, and Recall for each drone:

- 239 • Drone A → 95.6%, 96.4% e 91.9%;
- 240 • Drone B → 92.4%, 91.3% e 88.6%;
- 241 • Drone C → 88.7%, 87.1% e 82.8%.

242 The confusion matrix results, obtained through Roboflow,  
243 represent the outcomes derived from the train set of each  
244 dataset. The values in the rows represent the ground truth,  
245 while the values in the columns represent the prediction

	Car	House	Tree	False Neg.
Car	2383	0	0	165
House	0	66	0	20
Tree	0	0	269	15
False Pos.	50	60	0	0

Table 1: Confusion Matrix of Train Set of Drone A

	Car	House	Tree	False Neg.
Car	3508	0	0	1291
House	0	126	0	58
Tree	0	0	1780	219
False Pos.	94	26	8	0

Table 2: Confusion Matrix of Train Set of Drone B

	Car	House	Tree	False Neg.
Car	195	0	0	2
House	0	6	0	2
Tree	0	0	980	421
False Pos.	1	2	137	0

Table 3: Confusion Matrix of Train Set of Drone C

246 Finally, in addition to the three drones, a Master drone  
247 was constructed. The Master Drone is designed to manage  
248 and analyze identification data obtained from the drones (A,  
249 B, and C). The class initializes variables to store drone data  
250 and counts the occurrences of identified objects, such as cars,  
251 houses, and trees, from each drone. It then categorizes these  
252 counts based on the drone source and the type of identified  
253 object.

254 The class employs a systematic approach to aggregate  
255 identification data from each drone, taking collision scenarios  
256 into account. It utilizes methods to handle potential collisions,  
257 ensuring the accuracy of data representation. The collision resolution strategy  
258 considers confidence levels of identified objects and selectively updates the master list to avoid  
259 redundancy. For this selective update, the master will calculate  
260 the best identification between the drone who identified first and the one who is identifying, with the following equation:  
261 confidence of the identification multiplied by the drone  
262 reputation, all of the actual drone.

265 The code also features supporting mechanisms for collision  
266 detection, collision feasibility assessment, and evaluation  
267 of confidence levels. These mechanisms contribute to  
268 the systematic management of identification data from multiple  
269 drones, allowing for effective collision resolution and  
270 maintaining data integrity.

## 271 6 Experiments

272 In this experiment, our aim is to observe the outcomes resulting  
273 from the alteration of the reputation value for each drone  
274 across three distinct environments.

- 275 • Environment A - Primarily comprised of cars within a  
276 park.
- 277 • Environment B - Primarily comprised of additional  
278 houses.
- 279 • Environment C - Primarily comprised of an increased  
280 number of trees.

281 In this section, we will conduct two types of experiments.  
282 The first involves simulating both the drones and the master  
283 in the previously characterized three different environments,  
284 employing three distinct combinations of reputations. In the  
285 second experiment, we will once again simulate the agents  
286 in the three varied environments, systematically exploring all  
287 possible combinations of reputations among the drones.

288 With the alteration of each drone's reputation, our primary  
289 focus is to study how many identifications each drone can  
290 successfully accomplish. In the upcoming subsections, each  
291 experiment will be scrutinized in greater detail, elucidating  
292 the specific objectives of each.

### Environment A

293



Figure 1: Test A  
[18]

294 In this setting, a multitude of automobiles populate a parking  
295 lot, surrounded by a sparse scattering of trees, conspicuously  
296 devoid of any residential structures.

### Environment B

297



Figure 2: Test B  
[8]

298 This environment is balanced in the sense that it encompasses  
299 a diverse array of elements. It features a mix of houses, cars,  
300 and a smattering of trees.

301 **Environment C**



Figure 3: Test C  
[16]

302 This environment is primarily characterized by an abundance  
303 of trees, with a solitary dwelling in its midst.

304 **6.1 Experiment Setup 1**

305 In this initial experiment, our goal is to simulate the agents in  
306 designated environments, conducting three distinct tests and  
307 permuting the reputation values of each drone three times, as  
308 illustrated in the table below.

	A	B	C
Test A	25%	25%	75%
Test B	25%	75%	25%
Test C	75%	25%	25%

Table 4: Description of the tests

309 With this, our aim is to study and analyze the number of  
310 identifications each drone can accomplish under a specific  
311 reputation, taking into account the considerations made by  
312 the master. The various types of identifications include cars,  
313 houses, and trees, with the caveat that the master will only  
314 accept identifications with a confidence level equal to or ex-  
315 ceeding 51%.

316 **6.2 Experiment Setup 2**

317 In the second experiment, our objective is to revisit the effects  
318 of altering the reputation values of each drone, considering all  
319 possible permutations. The stages to be described encompass  
320 five intervals (0%, 25%, 50%, 75%, 100%) across the pre-  
321 viously mentioned three distinct environments. This results  
322 in 125 possible permutations. It is important to recall that the  
323 master will only accept identifications with a confidence level  
324 equal to or exceeding 51%.

325 **7 Results**

326 In this section, we aim to present the results obtained for each  
327 experiment after conducting simulations of the agents in the  
328 three aforementioned environments.

329 **7.1 Experiment Setup 1**

330 As previously stated in this initial experiment, our objective  
331 was to examine the outcomes resulting from the alteration of  
332 each drone's reputation values for three permutations.

333 **Environment A**

334 The results for Environment A are depicted in the table below  
335 as Figure 5.

	Cars	Houses	Trees
Drone A (25%)	114	0	0
Drone B (25%)	7	0	0
Drone C (75%)	176	0	0

Table 5: Environment A - Test A

336 For Drone A (25% reputation), there were 114 cars ob-  
337 served and no houses or trees. Drone B (25% reputa-  
338 tion) detected 7 cars with no houses or trees. Drone C (75% repu-  
339 tation) observed 176 cars with no houses or trees.

	Cars	Houses	Trees
Drone A (25%)	116	0	0
Drone B (75%)	155	0	0
Drone C (25%)	12	0	0

Table 6: Environment A - Test B

340 For Drone A (25% reputation), there were 116 cars ob-  
341 served and no houses or trees. Drone B (75% reputa-  
342 tion) detected 155 cars with no houses or trees. Drone C (25% repu-  
343 tation) observed 12 cars with no houses or trees.

	Cars	Houses	Trees
Drone A (75%)	300	0	0
Drone B (25%)	7	0	0
Drone C (25%)	8	0	0

Table 7: Environment A - Test C

344 For Drone A (75% reputation), there were 300 cars ob-  
345 served and no houses or trees. Drone B (25% reputa-  
346 tion) detected 7 cars with no houses or trees. Drone C (25% repu-  
347 tation) observed 8 cars with no houses or trees.

348 **Environment B**

349 The results for Environment B are depicted in the table below  
350 as Figure 6.

	Cars	Houses	Trees
Drone A (25%)	0	9	0
Drone B (25%)	0	0	0
Drone C (75%)	6	0	1

Table 8: Environment B - Test A

351 For Drone A (25%), there were 0 cars, 9 houses, and 0 trees  
352 observed. Drone B (25%) detected 0 cars with no houses or

353 trees. Drone C (75%) observed 6 cars with no houses and 1  
 354 tree, and did not detect any houses.

	Cars	Houses	Trees
Drone A (25%)	0	8	0
Drone B (75%)	0	3	0
Drone C (25%)	4	0	1

Table 9: Environment B - Test B

355 For Drone A (25%), there were 0 cars, 8 houses, and 0  
 356 trees observed. Drone B (75%) detected 0 cars, 3 houses, and  
 357 0 trees. Drone C (25%) observed 4 cars, 0 houses, and 1 tree.

	Cars	Houses	Trees
Drone A (75%)	0	10	0
Drone B (25%)	0	1	0
Drone C (25%)	4	0	1

Table 10: Environment B - Test C

358 For Drone A (75%), there were 0 cars, 10 houses, and 0  
 359 trees observed. Drone B (25%) detected 0 cars, 1 house, and  
 360 0 trees. Drone C (25%) observed 4 cars, 0 houses, and 1 tree.

### Environment C

361 The results for Environment C are depicted in the table below  
 362 as Figure 7.

	Cars	Houses	Trees
Drone A (25%)	0	1	0
Drone B (25%)	0	0	0
Drone C (75%)	0	0	7

Table 11: Environment C - Test A

364 For Drone A (25%), there were 0 cars, 1 house, and 0 trees  
 365 observed. Drone B (25%) detected 0 cars, 0 houses, and 0  
 366 trees. Drone C (75%) observed 0 cars, 0 houses, and 7 trees.

	Cars	Houses	Trees
Drone A (25%)	0	1	0
Drone B (75%)	0	0	0
Drone C (25%)	0	0	7

Table 12: Environment C - Test B

367 For Drone A (25%), there were 0 cars, 1 house, and 0 trees  
 368 observed. Drone B (75%) detected 0 cars, 0 houses, and 0  
 369 trees. Drone C (25%) observed 0 cars, 0 houses, and 7 trees.

	Cars	Houses	Trees
Drone A (75%)	0	1	0
Drone B (25%)	0	0	0
Drone C (25%)	0	0	7

Table 13: Environment C - Test C

For Drone A (75%), there were 0 cars, 1 house, and 0 trees  
 observed. Drone B (25%) detected 0 cars, 0 houses, and 0  
 trees. Drone C (25%) observed 0 cars, 0 houses, and 7 trees.

## 7.2 Experiment Setup 2

To obtain the results for this experiment, the RapidMiner tool  
 was employed to generate the graphs. Each graph consists of  
 the reputation of each drone on the X-axis, while the Y-axis  
 represents the average of all identifications made by a drone.  
 The graph is interpreted as follows: for instance, when drone  
 A has a reputation of 25%, the average number of identifica-  
 tions made by it across all possible reputation permutations is  
 represented by the value X

## 7.3 Environment A

The figure illustrating the results obtained in this environment  
 is located in the attached sheets (Figure 5). The table illus-  
 trates the various averages of identifications made by each  
 drone in environment A, taking into consideration all possi-  
 ble permutations.

## 7.4 Environment B

The figure illustrating the results obtained in this environment  
 is located in the attached sheets (Figure 6). The table illus-  
 trates the various averages of identifications made by each  
 drone in environment B, taking into consideration all possi-  
 ble permutations.

## 7.5 Environment C

The figure illustrating the results obtained in this environment  
 is located in the attached sheets (Figure 7). The table illus-  
 trates the various averages of identifications made by each  
 drone in environment C, taking into consideration all possi-  
 ble permutations.

## 8 Discussion

In this section, our intention is to discuss the results obtained  
 in each experiment and within each environment.

### Experiment Setup 1

In Experiment 1, the detailed analysis of each specific case  
 with the provided reputation combinations (25%, 25%, 75%),  
 (25%, 75%, 25%), and (75%, 25%, 25%) proved to be instru-  
 mental in accurately identifying the consequences of reputa-  
 tion changes in each drone. It became evident that scrutiniz-  
 ing individual cases allowed us to discern the impact of reputa-  
 tion alterations. Indeed, we observed a notable trend where  
 identification values increased for the drone with the highest  
 reputation among the three, and conversely, decreased when  
 reducing the reputation value.

For the test cases in Environment A, this correlation was  
 particularly pronounced. Additionally, it is intriguing to note  
 that while drone A maintained a reputation level of 25%, it  
 never dropped below 114 identifications of cars. This obser-  
 vation suggests that the model of drone A demonstrated  
 exceptional performance during training.

Similarly, in the test cases for Environment B, we observed  
 the same correlation. However, for the test cases in Environ-  
 ment C, no significant changes were obtained. This can be

423 attributed to the fact that the only model trained with a more  
424 extensive and improved dataset of trees belonged to drone C.  
425 Therefore, it is normal that the identification values in each  
426 permutation remain unchanged.

## 427 Experiment Setup 2

428 In this second experiment, through a detailed analysis of the  
429 obtained graphs, we were able to observe that, regardless of  
430 the reputation of each drone in each permutation, the average  
431 identifications for a given reputation X do not significantly alter  
432 the final outcome. For instance, in the cases involving the  
433 utilization of environment A, it became evident that Drone  
434 A consistently outperformed the average identifications made  
435 by other drones, irrespective of its reputation in any permutation.  
436 This observation is particularly intriguing given that,  
437 in the preceding experiment, the opposite trend was identified,  
438 wherein reputation had a discernible impact on the results.  
439 The findings underscore the importance of considering  
440 contextual nuances and specific environmental conditions in  
441 evaluating the influence of drone reputation on identification  
442 outcomes.

443 Additionally, in the test cases conducted in environment  
444 B, we observed the same relationship as mentioned earlier.  
445 Interestingly, and unexpectedly, Drone A demonstrated superior  
446 identification of houses compared to Drone B, which was  
447 supposedly anticipated to excel in identifying these types of  
448 objects. This unexpected outcome prompts further investigation  
449 into the factors influencing drone performance in different  
450 environments and under varying reputational permutations.

## 452 9 Conclusions

453 In this section, our aim is to present our conclusions drawn  
454 from the conducted experiments and elucidate their implications.

455 Commencing with the initial experiment, we successfully  
456 ascertained that the variation in the reputation value of each  
457 drone can indeed impact the number of identifications made  
458 within a given environment, as expounded in the Experiment  
459 1 section. The data unequivocally supports the veracity of  
460 this assertion. Furthermore, Experiment 1 revealed that, up to  
461 a certain threshold, the precision and accuracy of the agent's  
462 model may not be of paramount importance. Instead, the  
463 degree of reliance placed by the master on the said agent  
464 emerges as a critical determinant, as demonstrated by our  
465 findings.

466 However, in contrast, Experiment 2 yielded an intriguing  
467 revelation. It is noteworthy to analyze that if the master were  
468 afforded the opportunity to scrutinize all possible permutations  
469 of reputations in a real-world context, perhaps this agent  
470 would not attribute significant importance to the reputation  
471 factor. Additionally, Experiment 2 underscored that the crux  
472 for achieving a substantial number of identifications lies in  
473 the efficacy of the drone/agent's training, emphasizing the  
474 pivotal role played by precision and accuracy metrics.

475 In conclusion, within a real-world context featuring a  
476 multi-agent system, it may be prudent for the master agent,  
477 in an initial phase, to take into account the reputation of each  
478 slave agent, particularly when the master lacks knowledge of

479 the specific metrics associated with each agent. In such a scenario,  
480 the significance of the reputation factor would be solely contingent  
481 upon this informational gap. However, if the master has access to the precision and accuracy values of each  
482 agent, the reputation factor becomes inconsequential. This  
483 suggests that, when armed with comprehensive performance  
484 metrics, the master's decision-making process can be more effectively guided by the intrinsic capabilities of the individual agents rather than relying on reputation alone.

## 485 Limitations

486 **Limited Test History Retention:** A significant limitation of  
487 the current system is the absence of a memory mechanism  
488 within the master agent to record the number of accurate identifications  
489 made by the drones in past tests. The system lacks  
490 the capability to retain a historical record of the drones' performance,  
491 hindering the potential for a more comprehensive analysis of their learning trends over time. This limitation  
492 may impede the ability to assess the long-term effectiveness  
493 of individual drones and identify areas for targeted improvement.

494 **Absence of Confidence Level Assignment:** The master  
495 agent relies solely on reputation values without attributing  
496 confidence levels to the drones based on their performance  
497 in previous tests. This limitation means that the system does  
498 not utilize the valuable information gained from the historical  
499 accuracy of identifications to refine the level of trust assigned  
500 to each drone's outputs. Introducing a mechanism to incorporate  
501 confidence levels could enhance the system's ability to  
502 make nuanced decisions, particularly when faced with varying  
503 degrees of reliability in drone identifications.

504 **Overlapping Identifications Constraint:** The implemented  
505 system ensures that identifications within each test  
506 environment do not overlap with one another. While this design  
507 choice promotes clarity and avoids redundancy in the  
508 output, it introduces a limitation in terms of adaptability. The  
509 system could benefit from an enhancement allowing users  
510 to adjust the percentage level of overlapping identifications.  
511 Such flexibility would enable the system to capture potentially  
512 missed correct identifications, providing a pathway for  
513 improvement and adaptation based on user preferences and  
514 experimental needs.

## References

- 521 [1] Aerialroofimages. Dataset for b - homes.  
522 https://universe.roboflow.com/aerialroofimages/  
523 aerial-roof-classification . Last acess: 08/12/2023,  
524 2023.
- 526 [2] Car detection. Dataset for b - cars. https:  
527 //universe.roboflow.com/car-detection-yp3a2/  
528 dronecardetector . Last acess: 08/12/2023, 2023.
- 529 [3] Diogo A. Rosário, João E.M. Raposo, Kete-  
530 van. Dataset for a. https://app.roboflow.com/  
531 universidade-de-coimbra-isopc/drone-a-tb89u/  
532 overview . Last acess: 08/12/2023, 2023.
- 533 [4] Diogo A. Rosário, João E.M. Raposo, Kete-  
534 van. Dataset for b. https://app.roboflow.com/  
535 universidade-de-coimbra-isopc/drone-b-xkvry/  
536 deploy/1 . Last acess: 08/12/2023, 2023.
- 537 [5] Diogo A. Rosário, João E.M. Raposo, Kete-  
538 van. Dataset for c. https://app.roboflow.com/  
539 universidade-de-coimbra-isopc/drone-c-hytd/  
540 deploy/5 . Last acess: 08/12/2023, 2023.
- 541 [6] ELPIDA ELEFTHERIADI. Dataset for a - cars.  
542 https://universe.roboflow.com/elpida-eleftheriadi/  
543 carpk-xk8e1 . Last acess: 08/12/2023, 2021.
- 544 [7] ELPIDA ELEFTHERIADI. Dataset for c - cars.  
545 https://universe.roboflow.com/elpida-eleftheriadi/  
546 carpk-xk8e1 . Last acess: 08/12/2023, 2021.
- 547 [8] Hannah Ward-Glenton. Figure 2: Test  
548 b. https://www.cnbc.com/2023/08/30/  
549 uk-home-sales-set-to-hit-their-lowest-since-2012-as-mortgage-sales-plummet.  
550 html . Last acess: 1/12/2023, 2023.
- 551 [9] Jacob Solawetz. An introduction to the coco  
552 dataset. https://blog.roboflow.com/coco-dataset/ .  
553 Last acess: 1/12/2023, 2020.
- 554 [10] Jacob Solawetz, Francesco. What is yolov8?  
555 the ultimate guide. https://blog.roboflow.com/  
556 whats-new-in-yolov8/ . Last acess: 1/12/2023,  
557 2023.
- 558 [11] James Gallagher. What is object detection?  
559 the ultimate guide. https://blog.roboflow.com/  
560 object-detection/ . Last acess: 1/12/2023, 2023.
- 561 [12] Keita, Zoumana. Yolo object detection ex-  
562 plained. https://www.datacamp.com/blog/  
563 yolo-object-detection-explained . Last acess: 1  
564 /12/2023, 2022.
- 565 [13] L. Macedo, M. Tavares, P. Gaspar and F. A.  
566 Cardoso. Uncertainty and novelty-based selec-  
567 tive attention in the collaborative exploration of  
568 unknown environments. https://www.cisuc.uc.pt/  
569 download-file/13716/xfUuNEQI4iMb6mq04YI2 .  
570 Last acess: 08/12/2023, 2011.
- 571 [14] LAB. Dataset for a - tree. https:  
572 //universe.roboflow.com/lab-03nki/  
573 trees-segmentation-xzuhq . Last acess:  
574 08/12/2023, 2023.
- 575 [15] lego. Dataset for c - homes. https:  
576 //universe.roboflow.com/lego/roofs\_of\_houses/  
577 browse?queryText=-class%3Anull+-class%  
578 3Ab+class%3ARoofsofhouses&pageSize=50&  
579 startingIndex=150&browseQuery=true . Last  
580 acess: 08/12/2023, 2022.
- 581 [16] Matthias Hauser. Figure 3: Test c.  
582 https://matthias-hauser.pixels.com/collections/  
583 aerial+views+drone+photography . Last acess: 1  
584 /12/2023, 2020.
- 585 [17] ofek. Dataset for a - homes. https://universe.  
586 roboflow.com/ofek/identification-of-roofs/  
587 browse?queryText=-class%3Anull+class%  
588 3Aroof&pageSize=50&startingIndex=0&  
589 browseQuery=true . Last acess: 08/12/2023,  
590 2022.
- 591 [18] PRADEEP87. Figure 1: Test a. https:  
592 //www.istockphoto.com/br/foto/vista-a%C3%  
593 A9rea-do-estacionamento-de-carro-aberto-na-cidade-de-kuala-  
594 C3%A1sia-gm987900966-267886745 . Last  
595 acess: 1/12/2023, 2018.
- 596 [19] Roboflow. Roboflow. https://docs.roboflow.com/ .  
597 Last acess: 1/12/2023, 2023.
- 598 [20] treeclassification. Dataset for b - tree.  
599 https://universe.roboflow.com/treeclassification/  
600 tree\_classification\_count\_v3 . Last acess:  
601 08/12/2023, 2022.
- 602 [21] weiqi fan. Dataset for c - tree. https://universe.  
603 roboflow.com/weiqi-fan-ygbdj/label\_tree . Last  
604 acess: 08/12/2023, 2022.

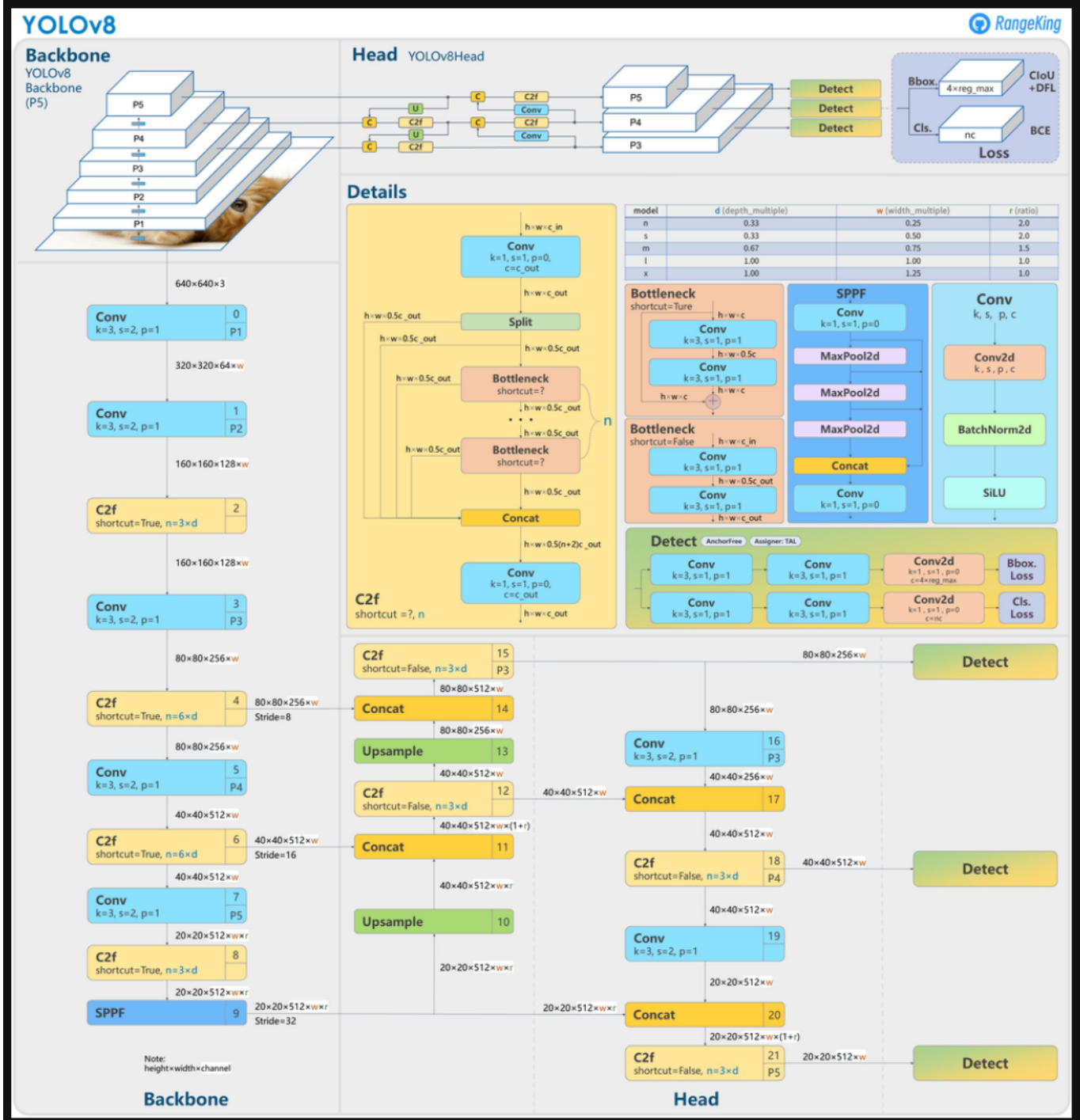


Figure 4: Yolov8 architecture

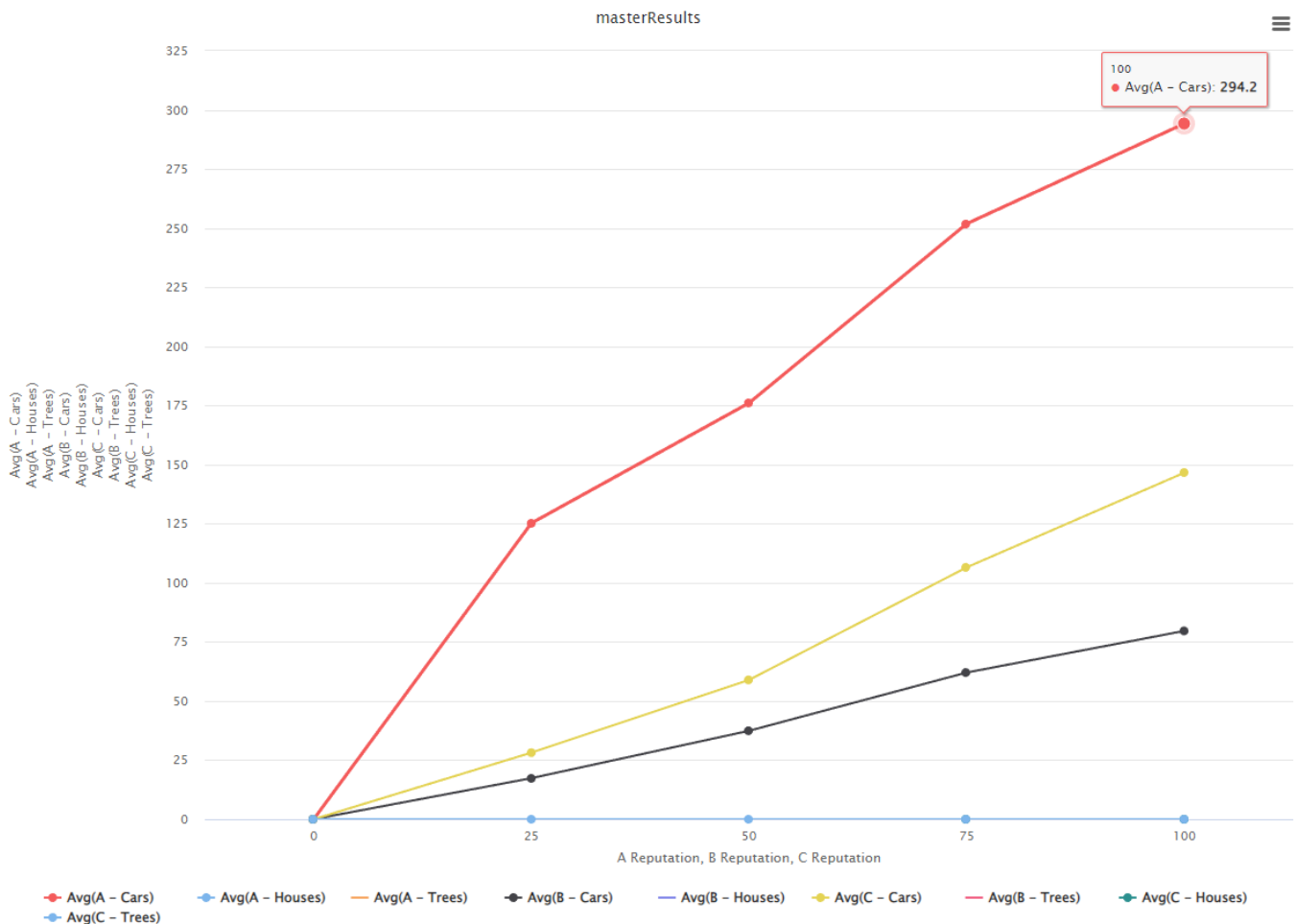


Figure 5: Test A results

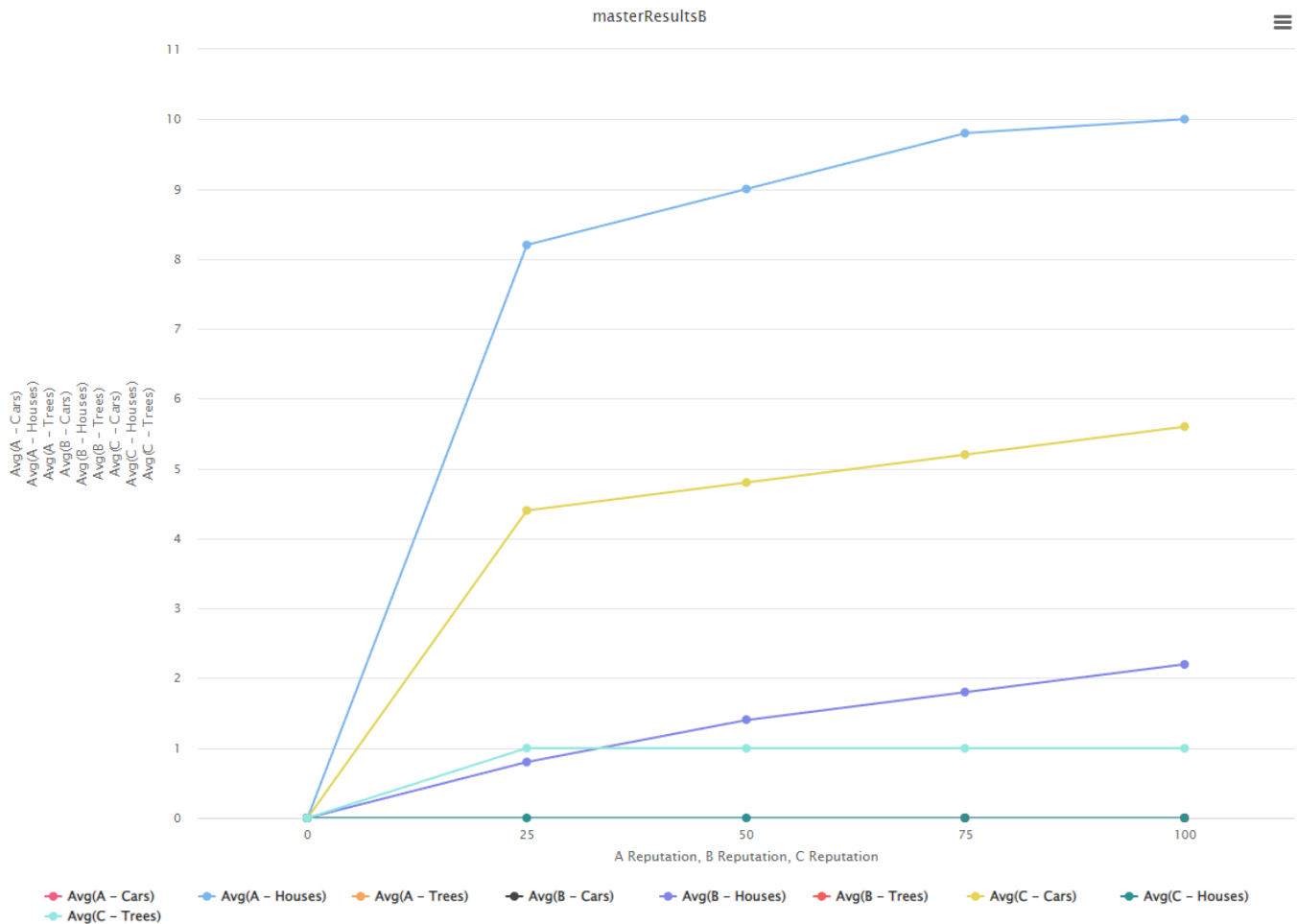


Figure 6: Test B results

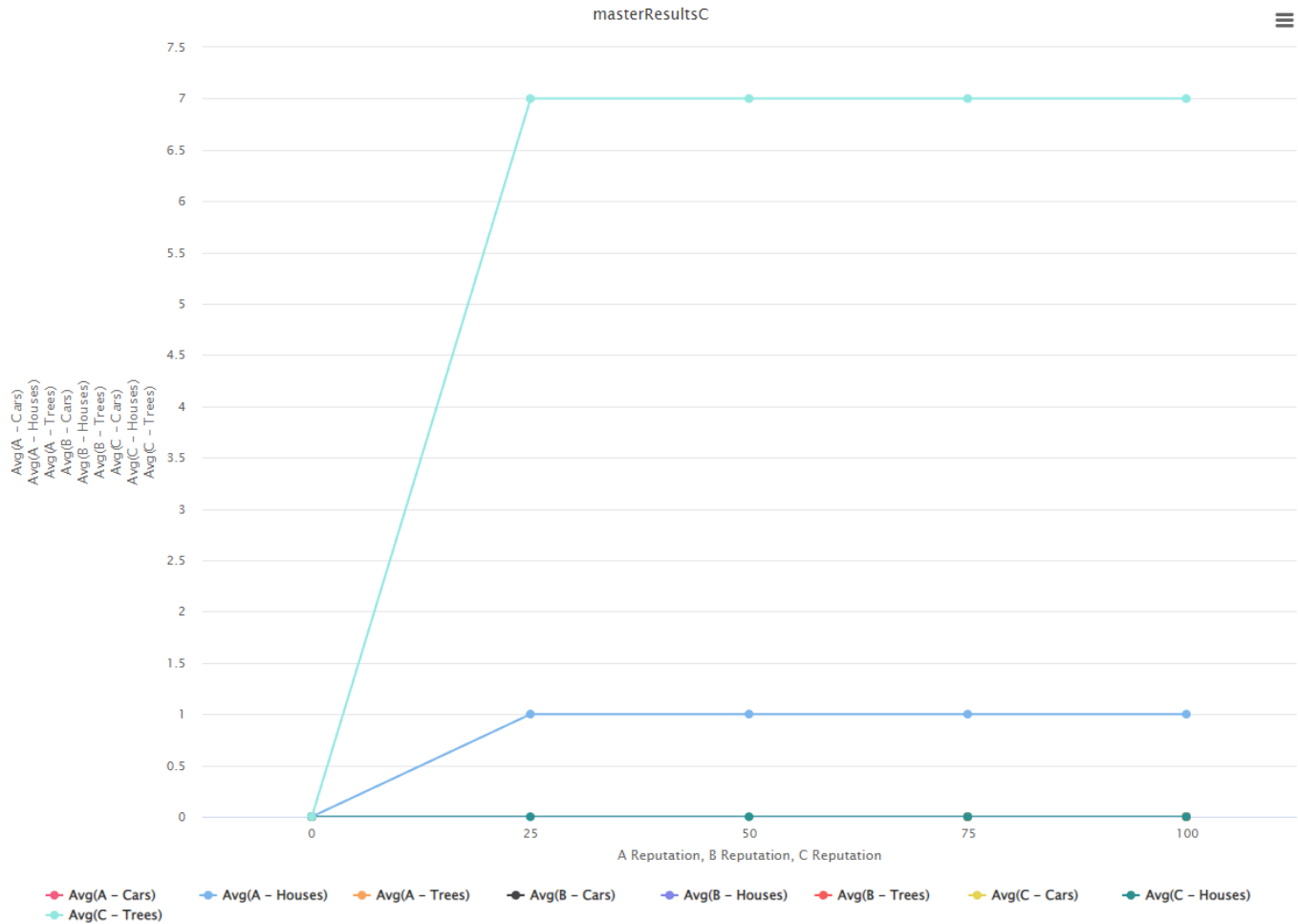


Figure 7: Test C results